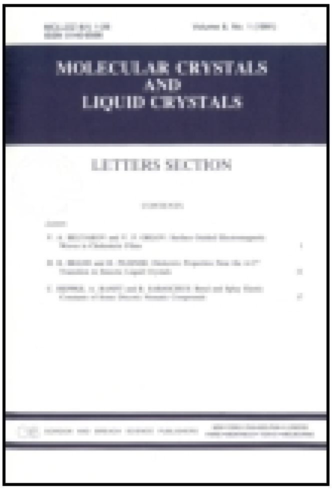

Molecular Crystals and Liquid Crystals
Publication details, including instructions for authors and subscription information:
http://www.tandfonline.com/loi/gmcl20

Synthesis and Characterization of Two Pb(II) Complexes of 2,2′-dihydroxy, Dimethoxy-1,1′-binaphthyl-3,3′-dicarboxylic Acid

Li-Jun Li[a], Chuan-Chuan Liu[a], Ming-Zhen Sun[a], Yu Qiao[a], Ying-Ying Huang[a] & Jian-Long Du[a]

[a] College of Chemistry and Environmental Science, and Chemical Biology Key Laboratory of Hebei Province, Hebei University, Baoding, P. R. China

Published online: 27 May 2014.

Mol. Cryst. Liq. Cryst., Vol. 593: pp. 187–200, 2014

ISSN: 1542-1406 print/1563-5287 online
DOI: 10.1080/15421406.2013.864547

Synthesis and Characterization of Two Pb(II) Complexes of 2,2′-dihydroxy, Dimethoxy-1,1′-binaphthyl-3,3′-dicarboxylic Acid

LI-JUN LI,* CHUAN-CHUAN LIU, MING-ZHEN SUN, YU QIAO, YING-YING HUANG, AND JIAN-LONG DU

College of Chemistry and Environmental Science, and Chemical Biology Key Laboratory of Hebei Province, Hebei University, Baoding, P. R. China

*Two new complexes {[Pb(**L**[1])(DMSO)$_2$(H$_2$O)]·DMF}$_n$ (**1**, **L**[1] = 2,2′-dihydroxy-l,l′-dinaphthyl-3,3′-dicarboxylate) and {[Pb(**L**[2])(DMS O)·DMSO}$_n$ (**2**, **L**[2] = 2,2′-dimethoxy-l,l′-dinaphthyl-3,3′-dicarboxylate) have been synthesized under mild conditions and structurally characterized. Crystal structural analysis reveals that complex **1** adopts a 1D infinite chain structure which forms 2D sheet by hydrogen bonds interactions. Complex **2** possesses a 2D sheet structure, which was further assembled into a 3D supramolecular network through the π-π weak interactions. IR spectra indicates the carboxyl group coordinates with the Pb^{2+} ion. TGA shows that complex **2** is highly thermally stable up to 120°C.*

Keywords Binaphthol-based ligands; crystal structure; metal-organic frameworks

Introduction

Metal-organic frameworks (MOFs), also called coordination polymer or coordination networks, are a class of hybrid materials formed by the self-assembly of metal ions or clusters and polydentate bridging ligands topically under mild conditions [1]. MOFs are unprecedentedly highly porosity, tunable, and can be built from a wide variety of inorganic connecting points and an infinite selection of organic bridging ligands. As a result, numerous MOFs have been engineered for different potential applications, including gas storage [2–4], chemical sensing [5–7], catalysis [8–10], and drug delivery [11, 12]. MOFs with large open channels are desired due to the large size of substrates and the resulting products. Unfortunately, MOFs with large open channels tend to undergo significant framework distortion upon the removal of solvent molecules, so it is still a challenge to construct the MOFs with large open channels.

The functionalization of binols has been investigated for several years. Such an interest is due to the great diversity of binaphthyl derivatives, which has been found a wide array of applications in many different areas of chemistry. Due to their axial chirality with *C2* symmetry and exhibiting a stable configuration in a broad range of conditions, binol derivatives have become important molecules in several fields [13, 14]. The binol core

*Address correspondence to Li-Jun Li, Key Laboratory of Chemical Biology of Hebei Province, Hebei University, Baoding 071002, China. Tel: +86 312 5079628; Fax.: +86 312 5079628. E-mail: llj@hbu.edu.cn

has been conveniently functionalized at both the 3,3′, 5,5′, and 6,6′ positions [15–18]. Furthermore, the access to the 4,4′ carbons has seldom been documented. Lin group have particularly demonstrated the utility of binaphthyl-derived MOFs in heterogeneous asymmetric catalysis [19, 20]. Although a number of strategies have been developed to achieve 2D or 3D structures MOFs in recent years [21], it is still a challenge to obtain MOFs with large open channels and extremely large porosity. Modification of the frameworks is still attracting much interest. Herein, we report two ligands $H_2\mathbf{L^1}$ and $H_2\mathbf{L^2}$ which have been synthesized and characterized. Two new complexes $\{[Pb(\mathbf{L^1})(DMSO)_2(H_2O)]\cdot DMF\}_n$ and $\{[Pb(\mathbf{L^2})\ (DMSO)]\cdot DMSO\}_n$ were obtained through the solvent diffusion conditions. We describe the synthesis, IR study, TGA and crystal structures of these complexes respectively.

Result and Discussion

IR Study

The infrared spectra shows that $\mathbf{H_2L^1}$ exhibits a very strong absorption at 1674 cm^{-1}, due to the asymmetrical vibration of the C=O of carboxyl group, but the absorption has disappeared in the infrared curve of complex **1**, owing to $\mathbf{H_2L^1}$ coordinates Pb^{2+} ion (Fig. 1a). The spectrum of complex **1** exhibits absorption at 1450 cm^{-1} and 1354 cm^{-1} corresponding with the asymmetrical and symmetrical vibrations of the carbonyl groups respectively. And more there is a wide and scattered band of phenolic hydroxyl from 2600 cm^{-1} to 3500 cm^{-1} (Fig. 1a). This assumed that the phenolic hydroxyl was uncoordinated with the metal ions, which assured the freedom of the active centers.

As shown in the Fig. 1b, the infrared curve of $\mathbf{H_2L^2}$ has a typical band of the asymmetrical and symmetrical vibrations of C−H of CH_3 are between 2840 cm^{-1} and 3076 cm^{-1} (Fig. 1b). And a strong absorption for the asymmetrical vibration of the C=O of carboxyl group appears at 1696 cm^{-1}, which has disappeared in the IR curve of complex **2** when the

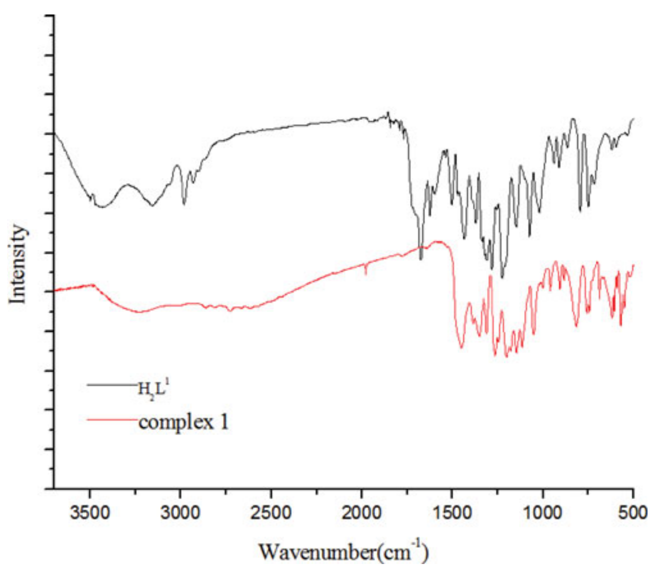

Figure 1a. IR spectra of $\mathbf{H_2L^1}$ and complex **1**.

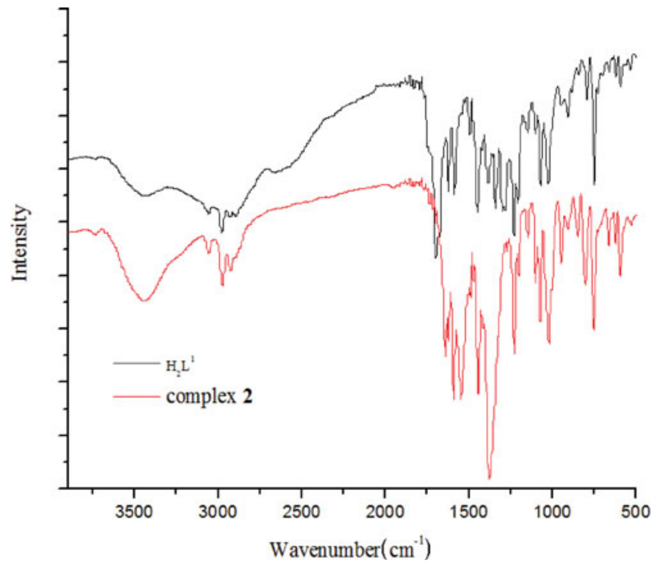

Figure 1b. IR spectra of $\mathbf{H_2L^2}$ and complex **2**.

$\mathbf{H_2L^2}$ coordinated Pb^{2+} ion (Fig. 1b). The spectrum of complex **2** exhibits absorption at $1543\ cm^{-1}$ and $1375\ cm^{-1}$ corresponding with the asymmetrical and symmetrical vibrations of the carbonyl groups respectively. According to IR, it is clear that metal ion coordinated carboxylate oxygen atoms, which is consistent with the analysis of crystal structure.,

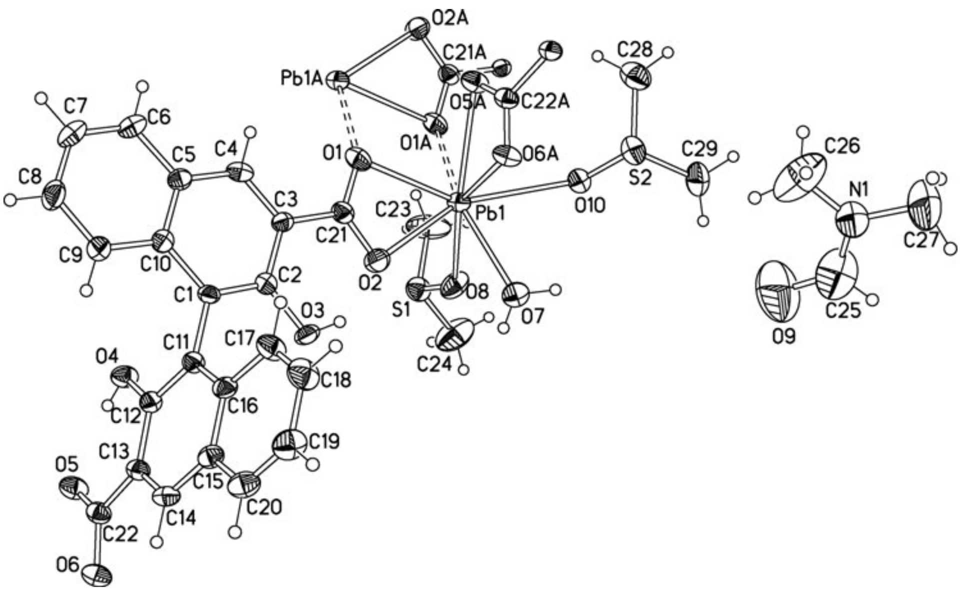

Figure 2a. The coordination environment around Pb(II) in complex **1** with the thermal ellipsoid at the 30% probability level. Symmetry code for complex **1**: #1 x+1,y,z, #2 x−1,y,z.

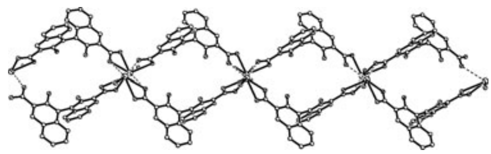

Figure 2b. The 1D spiral structure of complex **1**.

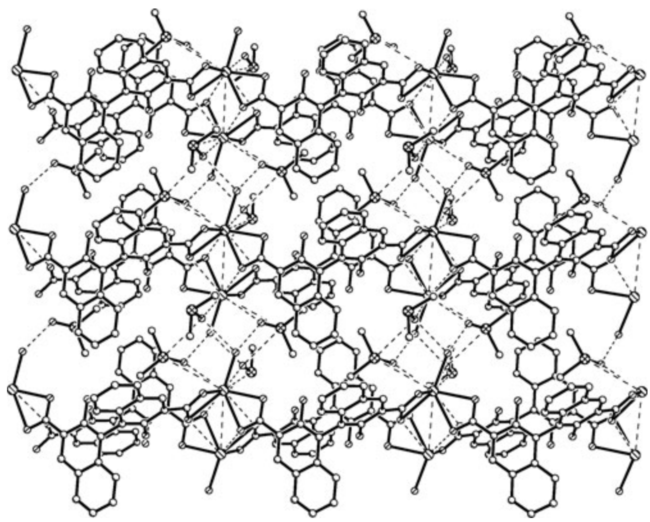

Figure 2c. The 2D layer structure of complex **1** formed by O–H···O interactions.

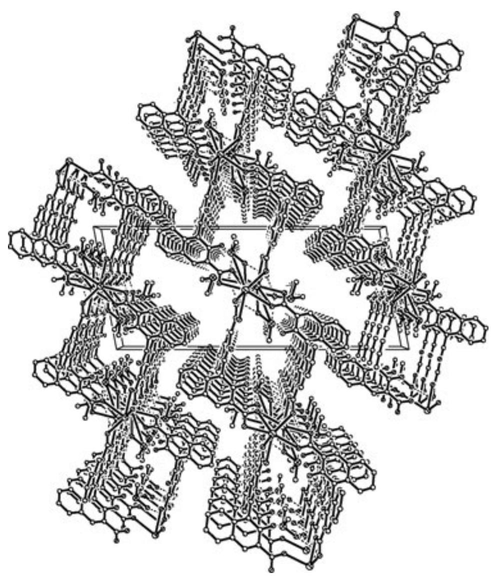

Figure 2d. The packing arrangement of **1**, viewed along *b*-axis.

Determination of Crystal Structure

Single crystal X-ray diffraction shows that complex **1** crystallizes in the Monoclinic space group P2(1)/c. There are one [Pb($\mathbf{L^1}$)(DMSO)$_2$(H_2O)] and one noncoordinated DMF guest molecules in the asymmetric unit of complex **1**. As shown in Fig. 2a, the Pb(II) ion exists in a distorted cubic geometry, being ligated by two μ2-carboxylate oxygen atoms and three common carboxylate oxygen atoms with the Pb-O distances between 2.423(4) Å and 2.687(4) Å, and two O atoms from DMSO, as well as a O atom from H_2O [Pb(1)-O(7) 2.528(5) Å]. The O-Pb-O angles range from 49.98(14)° to 127.21(14)°. The last DMF molecule is freely filled in the space of the unit. In complex **1**, the dihedral angle between the pair of naphthyl rings of the ligand is 77.27°, the ligands $\mathbf{H_2L^1}$ act as bridging molecules, which link the Pb^{2+} centers into an infinite lattice fence chain running along the a-axis (Fig. 2b). In addition, the adjacent 1D chains are assembled into a 2D network by the hydrogen bonds O(7)-H(7A)···O(10)$^{\#3}$, O(7)-H(7B)···S(1)$^{\#2}$, O(7)-H(7B)···O(8)$^{\#2}$ weak Interactions [H(7A)···O(10)$^{\#3}$ = 1.96 Å, H(7B)···S(1)$^{\#2}$ = 3.0 Å, H(7B)···O(8)$^{\#2}$ = 1.91 Å] (Fig. 2c).

Complex **2** crystallizes in Monoclinic space group P21/c. There are one [Pb($\mathbf{L^2}$)(DMSO)] and one noncoordinated DMSO guest molecule in the asymmetric unit of complex **2**. As shown in Fig. 3a, the Pb(II) is coordinated to five carboxylate oxygen atoms with the distance Pb-O between 2.321(6) and 2.675(5) Å, two O atoms from DMSO [Pb-O, 2.636(6) and 2.705(6) Å]. Furthermore the band length Pb(1)-O(1) [2.321(6) Å] is shorter than others. In complex **2**, the Pb(II) is in the center of pentagon defined by the donors atoms O(5)$^{\#1}$, O(2)$^{\#2}$, O(7), O(6)$^{\#1}$, and O(7)$^{\#2}$, while the O(1) and O(5)$^{\#3}$ occupy the apical positions to fulfill the distorted pentagonal bipyramid. The O-Pb-O angles are between 49.68(16)° and 165.76(19)°. The noncoordinated DMSO molecule is freely filled

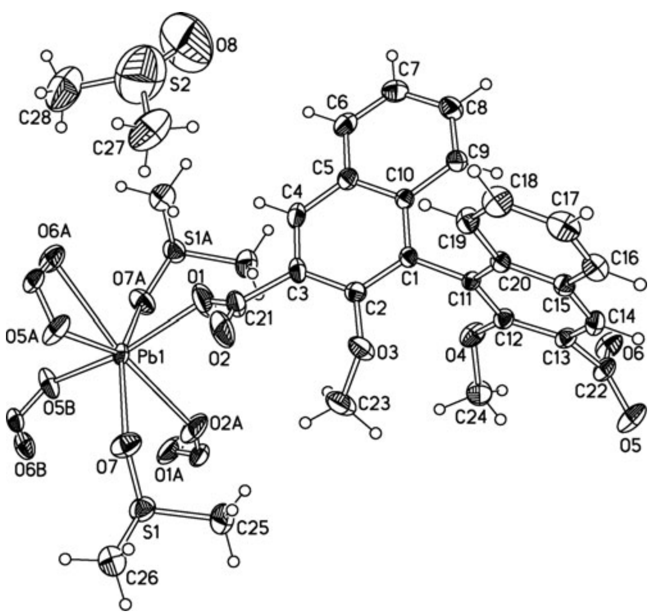

Figure 3a. The coordination environment around Pb(II) in complex **2** with the thermal ellipsoid at the 30% probability level. Symmetry code for complex **2**: #1 x+1, y, z; #2 x, −y+1/2, z−1/2; #3 x+1, −y+1/2, z−1/2; #4 x, −y+1/2, z+1/2; #5 x−1, y, z; #6 x−1, −y+1/2, z+1/2.

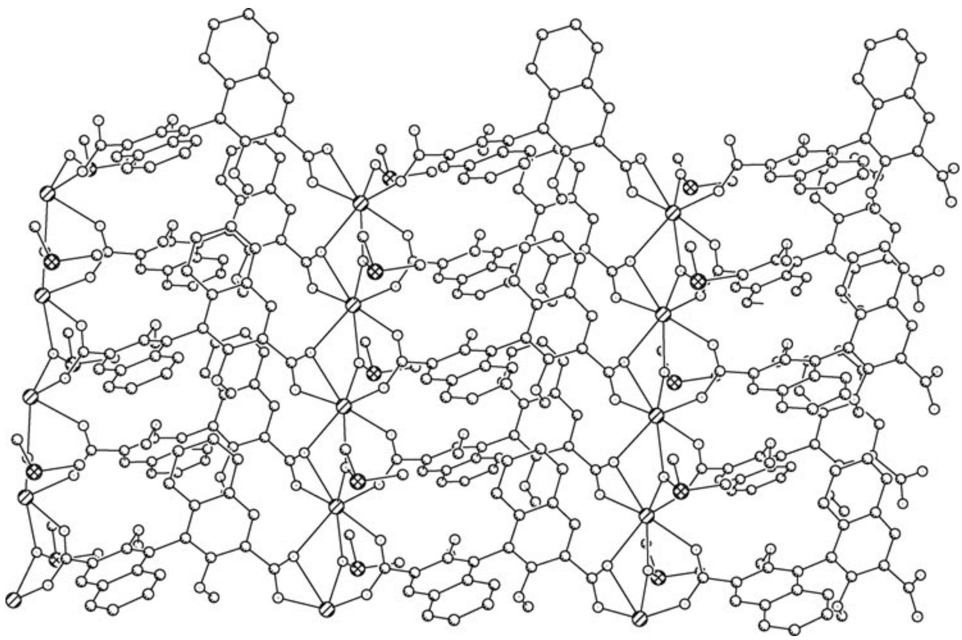

Figure 3b. The 2D layer structure of complex **2**.

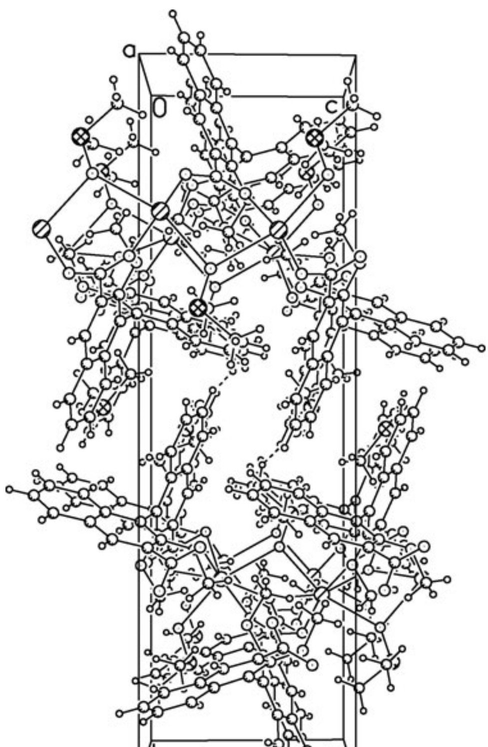

Figure 3c. The packing arrangement of complex **2**, viewed along the *a*-axis.

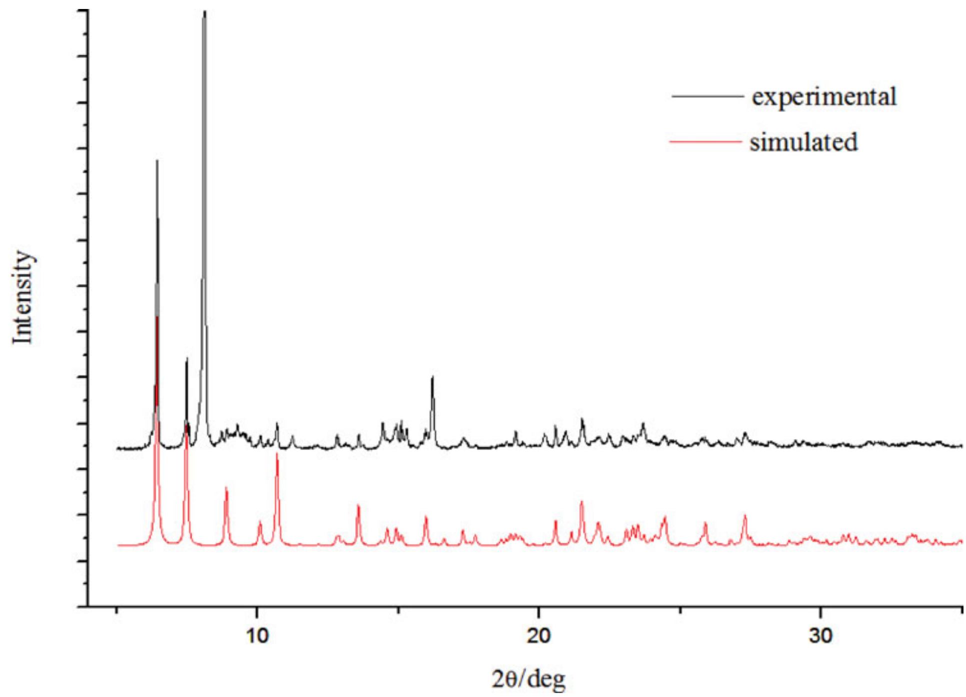

Figure 4a. Experimental and simulated XRPD patterns for complex **1**.

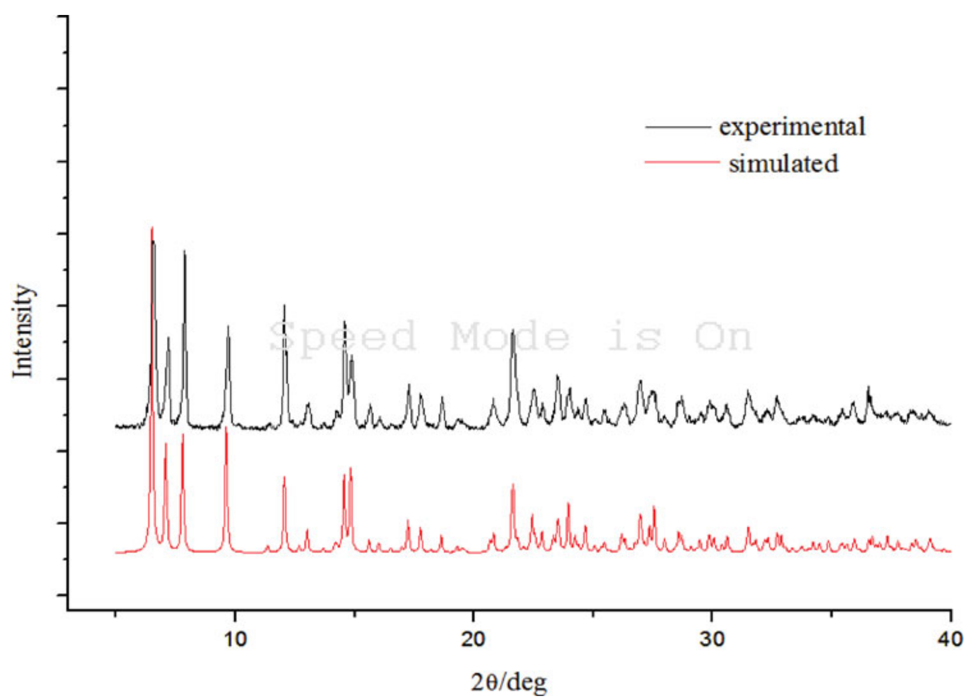

Figure 4b. Experimental and simulated XRPD pattern of complex **2**.

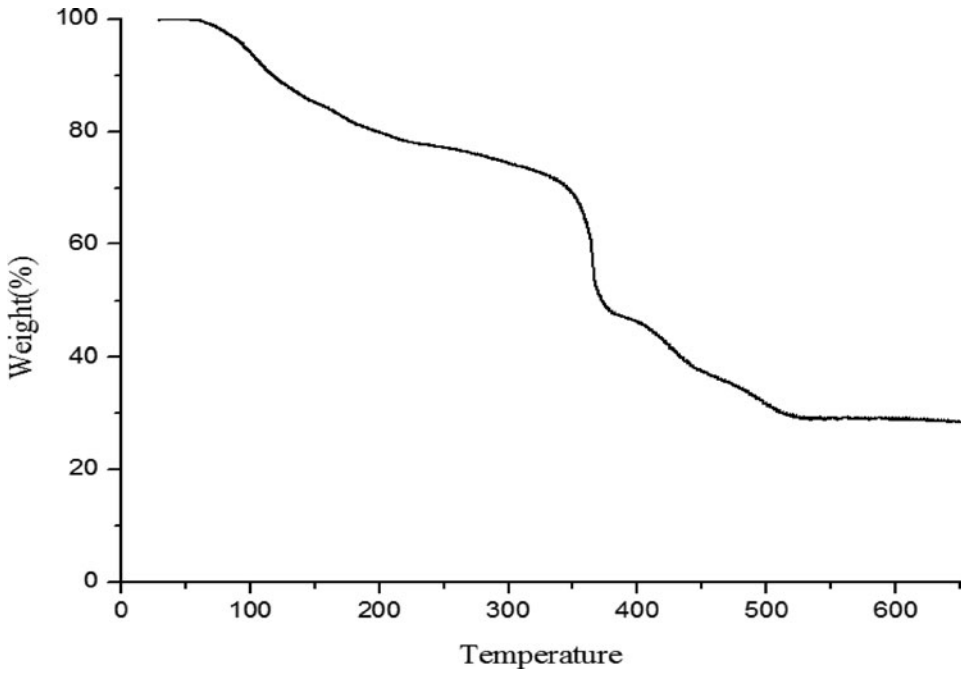

Figure 5a. The thermogravimetric curves of complex **1**.

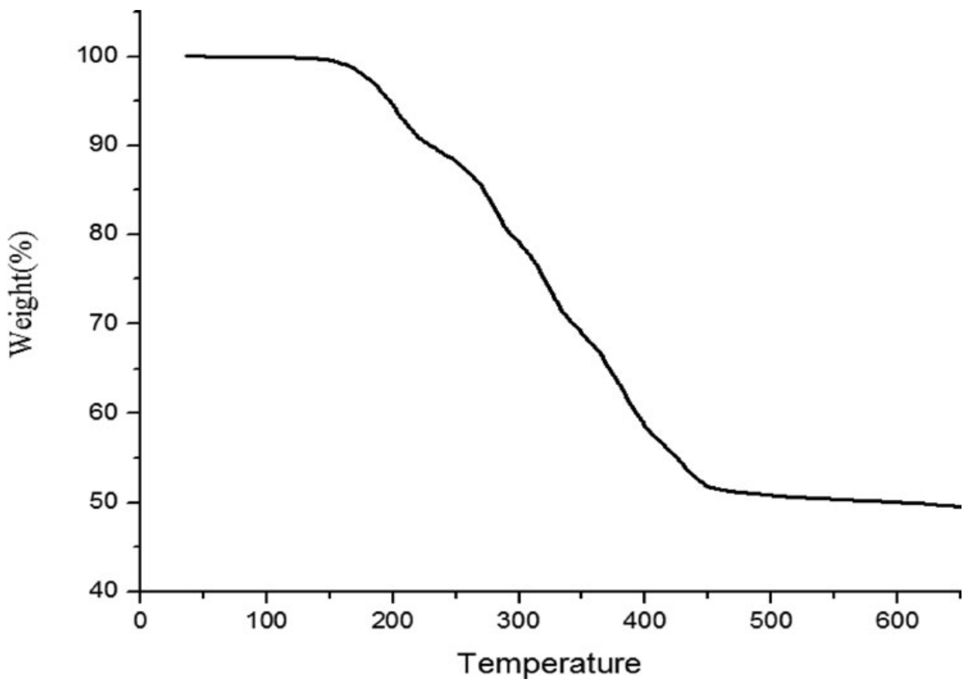

Figure 5b. The thermogravimetric curves of complex **2**.

Table 1. Crystal data and structure refinement parameters for complex **1** and complex **2**

Identification code	Complex **1**	Complex **2**
Empirical formula	$C_{29}H_{33}NO_{10}PbS_2$	$C_{28}H_{28}O_8PbS_2$
Formula weight	826.87	763.81
Temperature (K)	296(2)	173(2)
Wavelength (Å)	0.71073	0.71073
Crystal system	Monoclinic	Monoclinic
Space group	P2(1)/c	P21/c
Unit cell dimensions		
a (Å)	$a = 12.1204(16)$	$a = 12.507(3)$
b (Å)	$b = 9.2874(13)$	$b = 27.212(7)$
c (Å)	$c = 28.224(4)$	$c = 8.150(3)$
Volume(A^3)	3122.3(7)	2770.1(13)
Z	4	4
Calculated density (Mg/m^3)	1.759	1.832
Absorption coefficient (mm^{-1})	5.594	6.291
F(000)	1632	1496
Crystal size (mm)	0.26 × 0.07 × 0.05	0.34 × 0.28 × 0.11
Range for data collection	1.71–26.00°	2.21–27.00°
Reflections collected	16,883	16,171
Independent reflections	6136 ($R_{int} = 0.0312$)	6036 ($R_{int} = 0.0342$)
Refinement method	Full-matrix least-squares on F2	Full-matrix least-squares on F2
Data/restraints/parameters	6136/0/397	6036/1/358
Limiting indices	$-10<h<14$, $-11<k<11$, $-34<l<34$	$-7<h<15$, $-34<k<34$, $-10<l<10$
Goodness-of-fit on F2	1.163	1.036
Final *R* indices [$I > 2$sigma(I)]	$R^1 = 0.0380$, $wR^2 = 0.0858$	$R^1 = 0.0431$, $wR^2 = 0.0927$
R indices (all data)	$R^1 = 0.0522$, $wR^2 = 0.0888$	$R^1 = 0.0571$, $wR^2 = 0.0964$
Extinction coefficient	0.00044(7)	0.00044(7)
Largest diff. peak and hole (eA-3)	2.491 and −0.697	2.433 and −2.862

in the space of the unit. The dihedral angle between the pair of naphthyl rings of the ligand is 85.69° (close to right angle), and the $\mathbf{H_2L^2}$ act as the bridging ligands which link the Pb(II) center to form an infinite 2D planar structure (Fig. 3b) and further forms 3D framework because of π-π accumulation of aromatic ring.

X-ray Powder Diffraction

To confirm the phase purity of the bulk materials, the imitation, and actual measurement X-ray powder diffraction pattern of the complex **1** and complex **2** are showed at Fig. 4a and 4b. Although the experimental patterns of complex **1** and complex **2** have a few unindexed

Table 2a. Selected bond lengths (Å) and angles (°) for complex **1**. Symmetry code for complex **1**: #1 x+1,y,z, #2 x−1,y,z

Distances			
O(1)-Pb(1)	2.655(5)	O(2)-Pb(1)	2.550(4)
O(5)-Pb(1)$^{\#1}$	2.687(4)	O(6)-Pb(1)$^{\#1}$	2.423(4)
O(7)-Pb(1)	2.528(5)	Pb(1)-O(6)$^{\#2}$	2.423(4)
Pb(1)-O(5)$^{\#2}$	2.687(4)		
Angles			
C(22)-O(5)-Pb(1)$^{\#1}$	87.2(3)	C(22)-O(6)-Pb(1)$^{\#1}$	99.1(4)
Pb(1)-O(7)-H(7A)	111.7	Pb(1)-O(7)-H(7B)	112.6
O(6)$^{\#2}$-Pb(1)-O(7)	78.41(15)	O(6)$^{\#2}$-Pb(1)-O(2)	92.24(16)
O(7)-Pb(1)-O(2)	74.77(15)	O(6)$^{\#2}$-Pb(1)-O(1)	79.16(15)
O(7)-Pb(1)-O(1)	118.59(14)	O(2)-Pb(1)-O(1)	49.98(14)
O(6)$^{\#2}$-Pb(1)-O(5)$^{\#2}$	50.79(14)	O(7)-Pb(1)-O(5)$^{\#2}$	127.21(14)
O(2)-Pb(1)-O(5)$^{\#2}$	115.42(15)	O(1)-Pb(1)-O(5)$^{\#2}$	70.04(14)

Table 2b. Selected bond lengths (Å) and angles (°) for complex 2. Symmetry code for complex **2**: #1 x+1, y, z; #2 x, −y+1/2, z−1/2; #3 x+1, −y+1/2, z−1/2; #4 x, −y+1/2, z+1/2; #5 x−1, y, z; #6 x−1, −y+1/2, z+1/2

Distances			
Pb(1)-O(1)	2.321(6)	Pb(1)-O(7)$^{\#2}$	2.705(6)
Pb(1)-O(5)$^{\#1}$	2.534(5)	O(2)-Pb(1)$^{\#4}$	2.621(5)
Pb(1)-O(2)$^{\#2}$	2.621(5)	O(5)-Pb(1)$^{\#5}$	2.534(5)
Pb(1)-O(7)	2.636(6)	O(5)-Pb(1)$^{\#6}$	2.675(5)
Pb(1)-O(6)$^{\#1}$	2.646(5)	O(6)-Pb(1)$^{\#5}$	2.647(5)
Pb(1)-O(5)$^{\#3}$	2.675(5)	O(7)-Pb(1)$^{\#4}$	2.705(6)
Angles			
O(1)-Pb(1)-O(5)$^{\#1}$	91.3(2)	O(5)$^{\#1}$-Pb(1)-O(6)$^{\#1}$	49.68(16)
O(1)-Pb(1)-O(2)$^{\#2}$	89.1(2)	O(2)$^{\#2}$-Pb(1)-O(6)$^{\#1}$	165.76(19)
O(5)$^{\#1}$-Pb(1)-O(2)$^{\#2}$	144.39(19)	O(7)-Pb(1)-O(6)$^{\#1}$	117.72(16)
O(1)-Pb(1)-O(7)	95.7(2)	O(1)-Pb(1)-O(5)$^{\#3}$	152.2(2)
O(5)$^{\#1}$-Pb(1)-O(7)	68.08(16)	O(5)$^{\#1}$-Pb(1)-O(5)$^{\#3}$	108.8(2)
O(2)$^{\#2}$-Pb(1)-O(7)	76.45(19)	O(2)$^{\#2}$-Pb(1)-O(5)$^{\#3}$	85.5(2)
O(1)-Pb(1)-O(6)$^{\#1}$	88.1(2)	O(7)-Pb(1)-O(5)$^{\#3}$	109.42(18)
O(6)$^{\#1}$-Pb(1)-O(5)$^{\#3}$	90.51(18)	C(21)-O(2)-Pb(1)$^{\#4}$	141.2(5)
O(1)-Pb(1)-O(7)$^{\#2}$	87.1(2)	C(22)-O(5)-Pb(1)$^{\#5}$	95.9(4)
O(5)$^{\#1}$-Pb(1)-O(7)$^{\#2}$	136.22(17)	C(22)-O(5)-Pb(1)$^{\#6}$	144.4(5)
O(2)$^{\#2}$-Pb(1)-O(7)$^{\#2}$	79.4(2)	Pb(1)$^{\#5}$-O(5)-Pb(1)$^{\#6}$	104.64(17)
O(7)-Pb(1)-O(7)$^{\#2}$	155.61(19)	C(22)-O(6)-Pb(1)$^{\#5}$	90.8(4)
O(6)$^{\#1}$-Pb(1)-O(7)$^{\#2}$	86.54(17)	S(1)-O(7)-Pb(1)	121.6(3)
O(5)$^{\#3}$-Pb(1)-O(7)$^{\#2}$	65.11(16)	S(1)-O(7)-Pb(1)$^{\#4}$	135.8(3)
C(21)-O(1)-Pb(1)	132.4(6)	Pb(1)-O(7)-Pb(1)$^{\#4}$	101.07(18)

diffraction lines and some are slightly broadened in comparison with those simulated from the single-crystal model, they can still be well considered that the bulk synthesized material and the as-grown crystals are homogeneous for complex **1** and complex **2**, confirming their purity of phase.

Thermogravimetric Analysis

High thermal stability is an important precondition in the conversion of porous coordination frameworks. Thus, TGA of complex **1** and complex **2** have been performed in the temperature range 20–800°C at a rate of 10°C min^{-1} under N_2 atmosphere. As shown in Fig. 5a, thermogravimetric analysis (TGA) indicates that complex **1** is stable up to 65°C. The TG curve of complex **1** shows three weight loss steps. The first weight loss of 26.8% from 65°C to 321°C is corresponded to the loss of one guest DMF and two DMSO molecules. These results show that metal-DMSO bonds are weaker than metal-carboxyl bonds. The second weight loss of 26.2% between 321°C and 389°C is attributed to the loss of one water molecule and decomposition about a naphthyl ring of ligand. The last weight loss of 18% is attributed to decomposing another naphthyl ring and the residue is PbO.

Thermogravimetric curve of complex **2** (Fig. 5b)shows that complex **2** is much stable up to 120°C. The first weight loss is 10.1% in the range of 120°C–230°C, which ascribe to the loss of one DMSO molecule per formula unit (calculated 10.2%). And the involved DMSO molecule and half of the framework in two naphthyl rings become decomposed slowly with a further heating from 230°C to 460°C, remain finally constant fade away. The residue weight is 51%, which tentatively assigned these weights to the part of a naphthyl ring and PbO.

X-Ray Crystal-structure Analysis of Complexes

The single crystal data of the complexes was collected on a Bruker Smart Apex II CCD diffractometer using the graphite monochromated Mo K radiation (λ = 0.71073 Å). The data of complex **1** and complex **2** were collected at 296(2) K and 173(2) K. The structure was solved with a direct method and refined by full-matrix least-square methods using SHELXTL-97 program. All H atoms were placed geometrically. The crystallographic data and structure experimental details of the complexes were given in Table 1, and selected bond lengths and bond angles were presented in Table 2.

Conclusions

Two novel MOFs based on binol have been synthesized and characterized. IR spectra indicates the carboxyl group coordinates with the Pb^{2+} ion. Crystal structural analysis reveals that complex **1** adopts a 1D infinite line structure, the complex **1** is further assembled into a 2D supramolecular network through the hydrogen bonds. Complex **2** is 2D planar structure, which forms a 3D supramolecular network through π-π weak interactions. TGA shows that complex **2** is highly thermally stable up to 120°C. PXRD of complex **1** and complex **2** show their purity of phase. And this study shows that the metal ions and weak interactions play important roles in constructing the MOFs.

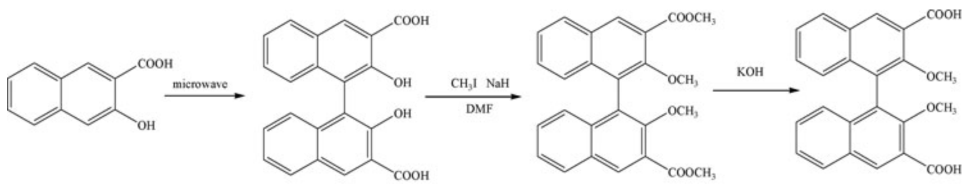

Scheme 1.

Experimental

All chemicals were purchased commercially and used without further purification. Infrared spectra were obtained with a Nicolet Impact 410 FTIR spectrometer in the range 400–4000 cm^{-1} using the KBr pellets. A Perkin-Elmer thermogravimetric analysis (TGA) thermogravimetric analyzer was used to obtain TGA curve in air with a heating rate of 20°C min^{-1}. ^{1}H NMR spectra were run at 25°C using a Bruker 600 (600 MHz) spectrometer. XRPD spectra were obtained with a Bruker D8 ADVANCE at 40 kV, 40 mA for a Cu-target tube and a graphite monochromator. Simulation of the XRPD spectra was carried out by the single-crystal data and the mercury 2.3 program.

The ligand $\mathbf{H_2L^1}$ is synthesized from 3-hydroxy-2-naphthoic acid through microwave coupling, and the $\mathbf{H_2L^2}$ is synthesized from $\mathbf{H_2L^1}$ through esterification and hydrolysis of the substrate (Scheme 1).

Synthesis of 2,2-dihydroxy-1,1-binaphthyl-3,3-dicarboxylic acid (H_2L^1)

$\mathbf{H_2L^1}$ was synthesized according to the published procedure.[22] A mixture of 3-hydroxy-2-naphthoic acid (9.4 g, 50 mmol) and $FeCl_3{\cdot}6H_2O$ (20.3 g, 56 mmol) was grinded, the mixture was conducted in microwave tube at 70°C and 500 W for 35 min. The mixture was kept at room temperature with occasional grinding for a certain period of the reaction time until the reaction was completed. The residue was purified by column chromatography on silica gel with petroleum ether/ethyl acetate (5:1) to afford the product $\mathbf{H_2L^1}$ (7.0 g, 74%, m.p. > 290°C). IR (KBr): 3059, 1661, 1499, 1455, 1272, 1228, 1150, 1072, 886, 796, and 736 cm^{-1}. ^{1}H NMR ($(CD_3)_2CO$, 600 MHz): δ 7.14–7.17 (m, 2H), 7.39–7.42 (m, 4H), 8.09–8.11 (m, 2H), and 8.84 (s, 2H). Anal. Calcd for $C_{22}H_{14}O_6$: C, 70.59; H,3.77. Found: C, 70.73; H,3.91%.

Synthesis of 2,2′-Dimethoxy-1,1′-Binaphthyl-3,3′-Dicarboxylic Acid Methyl Ester(2)

Compound **2** was synthesized according to the published procedure [23]. To a 50 mL three-necked round-bottom flask equipped with a magnetic stirrer and a reflux condenser was added $\mathbf{H_2L^1}$ (0.37 g, 1 mmol) and NaH (0.12 g, 2.62 mmol) in DMF (5 mL), the mixture was stirred at 50°C. Iodomethane (1.5 mL, 24 mmol) was slowly added after 1.5 h, and NaH (0.08 g, 1.78 mmol) was added into the mixture per hour. Tracking the reaction by TLC, until $\mathbf{H_2L^1}$ reacted completely. The resulting mixture was cooled to room temperature, and extracted with H_2O and ethyl acetate. The organic layer was dried over anhydrous $MgSO_4$ and the solvent was removed under reduced pressure. The solid residue was purified by column chromatography to afford the compound **2** (0.32 g, 70.3%. m.p.: 102–103°C), ^{1}H NMR($CDCl_3$, 600 MHz): δ 3.46 (s, 6H), 3.99 (s, 6H), 7.12–7.14 (d, J = 12 Hz, 2H), 7.31–7.36 (m, 2H), 7.43–7.46 (m, 2H), 7.96–7.98 (m, 2H), 8.54 (s, 2H); IR (KBr): 2943, 2840, 1726, 1620, 1590, 1497, 1444, 1412, 1350, 1304, 1280, 1231, 1206, 1152, 1075, 1005, 916, 799, and 750 cm^{-1}. Anal. Calcd for $C_{26}H_{22}O_6$: C, 72.55; H, 5.15. Found: C, 72.70; H, 5.26%.

Synthesis of 2,2′-dimethoxy-l,l′-dinaphthyl-3,3′- dicarboxylic acid (H_2L^2)

$\mathbf{H_2L^2}$ was synthesized according to the published procedure [24]. A solution of compound **2** (0.32 g, 0.70 mmol) in alcohol (2 mL) was added NaOH (5 mL, 10%) and stirred at 60°C for 10 hr, then removing the solvent under reduced pressure. the solution was acidified with hydrochloric acid to afford the $\mathbf{H_2L^2}$ as a white powder (0.244 g, 86.8% m.p.: 218–220°C). ^{1}H NMR (DMSO-d_6, 600 MHz): δ 3.42 (s, 6H), 6.97–6.99 (d, J = 12 Hz, 2H), 7.38 (t, J = 12 Hz, 2H), 7.48 (t, J = 12 Hz, 2H), δ 8.12–8.14 (d, J = 12 Hz, 2H), 8.54 (s, 2H,); IR (KBr): 2941, 2628, 1691, 1621, 1589, 1496, 1445, 1385, 1347, 1283, 1235, 1206, 1071, 1004, 907, 800, and 752 cm^{-1}. Anal. Calcd for $C_{24}H_{18}O_6$: C, 71.64; H, 4.51. Found: C, 71.80; H, 4.66%.

Synthesis of {[Pb(L^1)(DMSO)$_2$(H_2O)]·DMF}$_n$ (Complex 1)

A mixture of $\mathbf{H_2L^1}$ (7.5 mg, 0.02 mmol) and NaOH (1.6 mg, 0.04 mmol) was heated to dissolved in ethanol (5 mL). The solvent was evaporated and the residue was dissolved in DMF and DMSO (V:V = 1:1, 2 mL) as the under layer in a tube. DMSO, DMF, and H_2O (V:V:V = 1:1:3, 2 mL) were carefully layered as the middle layer. $Pb(NO_3)_2$ (6.6 mg, 0.02 mmol) was dissolved in DMF and H_2O (V:V = 1:1, 2 mL) as the up layer. The tube was then sealed. Diffusion between the three phases over a period produced transparent block pale yellow crystals of complex **1**. Anal. Calcd for $C_{29}H_{33}NO_{10}PbS_2$: C, 42.12; H, 4.02; N, 1.69. Found: C, 42.27; H, 4.11; N, 1.76%.

Synthesis of {[Pb(L^2)(DMSO)]·DMSO}$_n$ (Complex 2)

Complex **2** was obtained by the similar method as described for complex **1**. A mixture of $\mathbf{H_2L^2}$ (7.5 mg, 0.02 mmol) and NaOH (1.6 mg, 0.04 mmol) was warmed to dissolved in ethanol (5 mL). The solvent was evaporated and the residue was dissolved in DMSO (4 mL) as the under layer in a tube. DMSO and H_2O (V:V = 2:1, 3 mL) were carefully layered as the middle layer in the tube. $Pb(NO_3)_2$ (13.2 mg, 0.04 mmol) was dissolved in DMF and H_2O (V:V = 1:1, 4 mL) as the up layer. Diffusion between the three phases over a period produced white diamond crystals of complex **2**. Anal. Calcd for $C_{28}H_{28}O_8PbS_2$: C, 44.03; H, 3.69. Found: C, 44.15; H, 3.81%.

Acknowledgments

The work was financially supported by the Natural Science Foundation of Hebei Province (No. B2012201109, No. B2010000223), and Science & Technology Pillar Program of Hebei Province (No. 12211212). Crystallographic data for the structural analysis have been deposited with the Cambridge Crystallographic Data Centre, CCDC No. 949351 and 949350. Copies of this information can be obtained free of charge from The Director, CCDC, 12 Union road, Cambridge, CB21EZ, UK (fax: +44 1223 336033; E-mail: deposit@ccdc.cam.ac.ukor; www:http://www.ccdc.cam. ac.uk).

References

[1] Holliday, B. J., & Mirkin, C. A. (2001). *Angew. Chem., Int. Ed.*, *40*, 2022.
[2] Rowsell, J., & Yaghi, O. (2004). *Microporous Mesoporous Mater.*, *73*, 3.
[3] Chae, H. K., Siberio-Pérez, D. Y., Kim, J., Go, Y., Eddaoudi, M., Matzger, A. J., O'Keeffe, M., & Yaghi, O. M. (2004). *Nature*, *427*, 523.
[4] Bennett, M. V., Beauvais, L. G., Shores, M. P., & Long, J. R. (2001). *J. Am. Chem. Soc.*, *123*, 8022.
[5] Burdette, S. C., Walkup, G. K., Spingler, B., Tsein, R. Y., & Lippard, S. J. (2001). *J. Am. Chem. Soc.*, *123*, 7831.
[6] Jiang, L., Wang, L., Guo, M., Yin, G., & Wang, R.-Y. (2011). *Sens. Actuators, B*, *159*, 148.
[7] Lahav, M., Gabai, R., Shipway, A. N., & Willner, I. (1999). *Chem. Commun.*, 1937.
[8] Meek, S. T., Greathouse, J. A., & Allendorf, M. D. (2011). *Adv. Mater.*, *23*, 249.
[9] Corma, A., Garcia, H., & Xamena, F. X. L. (2010). *Chem. Rev.*, *110*, 4606.
[10] Seo, J. S., Wand, D., Lee, H., Jun, S. I., Oh, J., Jeon, Y., & Kim, K. (2000). *Nature*, *404*, 982.
[11] Rieter, W. J., Pott, K. M., Taylor, K. M. L., & Lin, W. B. (2008). *J. Am. Chem. Soc.*, *130*, 11584.
[12] Horcajada, P., Chalati, T., Serre, C., Gillet, B., Sebrie, C., Baati, T., Eubank, J. F., Heurtaux, D., Clayette, P., Kreuz, C., Chang, J. S., Hwang, Y. K., Marsaud, V., Bories, P. N., Cynober, L., Gil, S., Ferey, G., Couvreur, P., & Gref, R. (2010). *Nat. Mater.*, *9*, 172.
[13] Eddaoudi, M., Moler, D. B., Li, H. L., Chen, B. L., Reineke, T. M., O'Keeffe, M., & Yaghi, O. M. (2001). *Acc. Chem. Res.*, *34*, 319.
[14] James, S. L. (2003). *Chem. Soc. Rev.*, *32*, 276.
[15] Zhu, Y., Gergel, N., & Majumdar, N. (2006). *Org. Lett.*, *8*, 355.
[16] Yan, B. B., Xu, Y., Goh, N. K., *et al.* (2000). Hydrothemal synthesis and crystal structures of novel hybrid open frameworks and a two-dimensional network based on tungsten oxides[J]. *Chem. Commun.*, *43*, 2169.
[17] Koeckelberghs, G., Verbiest, T., & Vangheluwe, M. (2005). *Chem. Mater.*, *17*, 118.
[18] Richter, S. N., Maggi, S., & Palumbo, M. (2004) *J. Am. Chem. Soc.*, *126*, 13973.
[19] Wu, C. D., & Lin, W. B. (2007). *Angew. Chem. Int. Ed.*, *46*, 1075.
[20] Wu, C. D., Hu, A., & Zhang, L. (2005). *J. Am. Chem. Soc.*, *127*, 8940.
[21] Férey, G., Mellot-Draznieks, C., & Serre, C. (2005). *Acc. Chem. Res.*, *38*, 217.
[22] Vill, E. D., & Sauvaget, F. (1994). Dry synthesis under microwave irradiation: a rapid and efficient coupling of naphthols [J]. *Synlett*, *6*, 435.
[23] Reetz, M. T., Merk, C., & Mehler, G. (1998). *Chem. Commun.*, *19*, 2075.
[24] Li, L. J., Li, C. Z., Zhang, D. H., & Zang, J. C. (2009). *Chem. J. Internet.*, *11*, 515.